Neurobiology of Disease 170 (2022) 105769

Contents lists available at ScienceDirect

Neurobiology of Disease

journal homepage: www.elsevier.com/locate/ynbdi

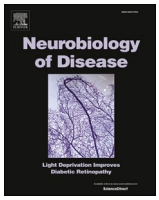

Directing LRRK2 to membranes of the endolysosomal pathway triggers RAB phosphorylation and JIP4 recruitment

Jillian H. Kluss [a,b,1], Luis Bonet-Ponce [a,1], Patrick A. Lewis [b,c,d], Mark R. Cookson [a,*]

[a] Cell Biology and Gene Expression Section, Laboratory of Neurogenetics, National Institute on Aging, National Institutes of Health, Bethesda, MD 20892-3707, USA
[b] School of Pharmacy, University of Reading, Whiteknights, Reading, UK
[c] Royal Veterinary College, Royal College Street, London, UK
[d] UCL Queen Square Institute of Neurology, Queen Square, London, UK

ARTICLE INFO

Keywords:
LRRK2
Parkinson's disease
Endolysosomal membranes

ABSTRACT

Coding mutations in the *Leucine-rich repeat kinase 2* (*LRRK2*) gene, which are associated with dominantly inherited Parkinson's disease (PD), lead to an increased activity of the encoded LRRK2 protein kinase. As such, kinase inhibitors are being considered as therapeutic agents for PD. It is therefore of interest to understand the mechanism(s) by which LRRK2 is activated during cellular signaling. Lysosomal membrane damage represents one way of activating LRRK2 and leads to phosphorylation of downstream RAB substrates and recruitment of the motor adaptor protein JIP4. However, it is unclear whether the activation of LRRK2 would be seen at other membranes of the endolysosomal system, where LRRK2 has also shown to be localized, or whether these signaling events can be induced without membrane damage. Here, we use a rapamycin-dependent oligomerization system to direct LRRK2 to various endomembranes including the Golgi apparatus, lysosomes, the plasma membrane, recycling, early, and late endosomes. Irrespective of membrane location, the recruitment of LRRK2 to membranes results in local accumulation of phosphorylated RAB10, RAB12, and JIP4. We also show that endogenous RAB29, previously nominated as an activator of LRRK2 based on overexpression, is not required for activation of LRRK2 at the Golgi nor lysosome. We therefore conclude that LRRK2 signaling to RAB10, RAB12, and JIP4 can be activated once LRRK2 is accumulated at any cellular organelle along the endolysosomal pathway.

1. Introduction

Multiple pathogenic mutations in the *Leucine-rich repeat kinase 2* (*LRRK2*) have been documented in families with ascertained autosomal dominant inheritance of Parkinson's disease (PD) (Funayama et al., 2005; Paisán-Ruíz et al., 2004; Zimprich et al., 2004). Additionally, due to incomplete age-dependent penetrance of *LRRK2* alleles, mutations are also associated with apparently sporadic PD (Gilks et al., 2005; Iwaki et al., 2020; Lee et al., 2017). Finally, non-coding variants in the promoter region of *LRRK2* are also risk factors for sporadic PD (Nalls et al., 2019). Thus, the genomic region encompassing *LRRK2* contains multiple types of genetic risk covering a range of identified modes of inheritance (Singleton and Hardy, 2011).

Because familial cases with LRRK2 mutations show clinical presentations that are indistinguishable from sporadic PD (Kumari and Tan, 2009, p. 2), it is reasonable to infer that the different types of LRRK2 variants work through common mechanisms. The most promising explanatory event uncovered to date is an increase in LRRK2 kinase activity, mediated either directly by mutation in the LRRK2 kinase domain or by decreased GTP hydrolysis, which is encoded by the adjacent Ras of complex proteins (ROC) and C-terminal of ROC (COR) bidomain (Cookson, 2010). All known pathogenic mutations identified to date increase either LRRK2 autophosphorylation at residue S1292 (Sheng et al., 2012) or on downstream Ras-associated binding proteins

Abbreviations: EHD1, EH domain-containing protein 1; FRB, FKBP-rapamycin binding domain; FKBP, FK506 binding protein; PD, Parkinson's disease; LAMP1, Lysosome-associated membrane glycoprotein 1; LRRK2, Leucine-rich repeat kinase 2; JIP4, JNK-interacting protein 4; PM, plasma membrane; PMTS, Plasma membrane-targeting sequence; RAB, Ras-associated binding protein.

* Corresponding author.
E-mail address: cookson@mail.nih.gov (M.R. Cookson).

[1] These authors contributed equally

https://doi.org/10.1016/j.nbd.2022.105769
Received 17 December 2021; Received in revised form 20 April 2022; Accepted 11 May 2022
Available online 14 May 2022

(RABs), including RAB10 and RAB12 (Steger et al., 2016). Non-coding variants likely influence disease risk by virtue of higher *LRRK2* gene expression, being an example of an expression quantitative trait locus (eQTL) (Ryan et al., 2017). An important corollary of these observations is that inhibition of LRRK2 might be clinically beneficial for inherited and, by extension, sporadic PD (Kluss et al., 2019; West, 2014).

Protein kinases are typically subject to regulation by multiple mechanisms within cellular signaling pathways, allowing for control of activity appropriate to internal or external cues. LRRK2 has been shown to be regulated in multiple cellular contexts. Inflammatory cell activation, which has been implicated in PD, has been shown to regulate LRRK2 phosphorylation, dimer formation and recruitment to intracellular membranes (Berger et al., 2010). We and others have also shown that lysosomal damage is sufficient to recruit LRRK2 to these organelles (Bonet-Ponce et al., 2020; Eguchi et al., 2018), which may be relevant to inflammatory signaling as exposure to specific intracellular pathogens can result in disruption of lysosomes (Herbst et al., 2020). Subsequent to lysosomal recruitment, LRRK2 phosphorylates RAB10 and RAB35 that are then able to recruit JNK-interacting protein 4 (JIP4), a motor adaptor protein, resulting in tubulation and sorting of lysosomal membranes, a process we termed LYTL (Bonet-Ponce et al., 2020). A related process may occur in neurons where pRAB10 can also recruit JIP4 to alter transport of autophagosomes along microtubules (Boecker et al., 2021).

Additionally, LRRK2 may be activated by interaction with RAB29, itself a candidate risk gene for sporadic PD (Nalls et al., 2019). Several groups have shown that overexpression of RAB29 can lead to LRRK2 recruitment to the Golgi apparatus (Beilina et al., 2020; Beilina et al., 2014) with downstream activation of RAB10 (Fujimoto et al., 2018; Liu et al., 2018; Purlyte et al., 2018). Of note, RAB29 overexpression has been reported to cause alteration of Golgi structure (Fujimoto et al., 2018), implying potential damage to this organelle. Interestingly, directing RAB29 to the mitochondrial membrane is also sufficient to activate LRRK2 signaling, suggesting that membrane identity is not important in LRRK2 activation pathways (Gomez et al., 2019). Additionally, whether RAB29 regulates LRRK2 in a physiological context has been questioned as knockout of RAB29 does not lower LRRK2-dependent phosphorylation of RAB10 in vivo (Kalogeropulou et al., 2020).

Here, we revisit the question of whether LRRK2 can be activated at particular membranes compared to others along the endolysosomal pathway, as well as whether membrane damage is necessary to activate LRRK2 once at the membrane. To do this, we utilized the rapamycin-binding domain from the 12 kDa FK506 binding protein (FKBP), which we fused to the N-terminus of LRRK2, and the FKBP-rapamycin-binding (FRB) domain of mTOR fused to six different membrane resident proteins (Liberles et al., 1997; Robinson et al., 2010). In the presence of rapamycin, the FKBP and FRB domains will dimerize, thus trapping LRRK2 to a specific membrane. In this manner, we recruited LRRK2 to the Golgi, lysosomes, recycling endosomes, early endosomes, late endosomes and plasma membrane. In each case we found evidence for accumulation of pRAB10 and pRAB12 and recruitment of JIP4 to the directed membrane in the absence of membrane damaging agents. Further, we confirmed that RAB29 is not required for LRRK2 activation at the Golgi nor lysosome by using an siRNA knockdown of endogenous RAB29, thus implying that the overexpression of RAB29 influences LRRK2 localization but the physical interaction is not needed for LRRK2 kinase activity at the membrane. The results underscore that LRRK2 can be activated at multiple *endo*-membranous compartments in cells and that this is sufficient to initiate downstream LRRK2 signaling.

2. Methods

2.1. Cell culture

HEK293FT cells were maintained in DMEM containing 4.5 g/l glucose, 2 mM L-glutamine, 5% Pen/Strep and 10% FBS at 37 °C in 5% CO_2. For immunocytochemistry experiments, cells were seeded on 12 mm coverslips (Corning, #354087). For Western blot experiments, cells were plated in 24-well plates. For all experiments, Matrigel coating (Corning, #354230) was used when seeding cells.

2.2. Reagents and treatments

For all experiments, rapamycin (Cayman Chemicals, cat #13346) was added at 200 nM in ethanol for 15 min before fixing or lysing cells for downstream analyses. Addition of MLi-2 (Tocris, cat #5756) was used at 1 μM in DMSO, 90 min prior to rapamycin treatment.

2.3. Cloning

FKBP sequence was tagged to 3xFLAG-pDEST and mScarlet-pDEST vectors using IN-FUSION HD cloning technology (Clontech, Takara, cat #638920). LRRK2-WT, LRRK2-R1441C, LRRK2-Y1669C, LRRK2-K1906M and LRRK2-G2019S, previously cloned into pCR™8/GW/TOPO™ vector (ThermoFisher, cat #250020), were transferred into the 3xFLAG-FKBP-pDEST and mScarlet-FKBP-pDEST plasmids using Gateway technology (ThermoFisher, cat #11791043). CFP-FRB-LAMP1 vector (Willett et al., 2017) was a gift from Rosa Puertollano (NIH). EHD1-FRB-GFP was kindly provided by Tsukasa Okiyoneda (Kwansei Gakuin University). iRFP-FRB-RAB5, iRFP-FRB-RAB7, and PM-FRB-CFP plasmids (Addgene plasmid #51612, #51613, and #67517) (Hammond et al., 2014; Varnai et al., 2006) were gifts from Tamas Balla (NIH). FRB-ECFP-Giantin was provided by Dorus Gadella (Addgene plasmid #67903) (van Unen et al., 2015).

2.4. Transfection and siRNA knockdown

Transient transfections of HEK293FT cells were performed using Lipofectamine 2000 in Gibco's Opti-MEM (ThermoFisher, cat #31985088). HEK293FT cells were transfected followed by a 24-h incubation period prior to any treatments, fixation, or lysis. The following concentrations were used for each construct: 0.4 μg for LRRK2, CFP-FRB-Giantin, and iRFP-FRB-RAB7, 0.25 μg for GFP-FRB-EHD1, CFP-FRB-LAMP1, and iRFP-FRB-RAB5, and 0.05 μg for CFP-FRB-PMTS. For endogenous RAB29 knockdown experiments, cells were treated with either non-targeting control siRNA or human RAB29 siRNA (40 nM working concentration) together with Lipofectamine RNAiMAX (ThermoFisher, cat #13778075) in Gibco's Opti-MEM and incubated for 24 h prior to starting the transfection protocol. We chose a 24-h incubation period as prior experiments suggest that this is sufficient time for robust protein expression in HEK293FT cells and, similarly, siRNA will result in efficient knockdown, at least for proteins with shorter half-lives, without inducing cellular toxicity.

2.5. Antibodies

The following primary antibodies were used: mouse anti-FLAG M2 (Sigma-Aldrich, cat #F3165, 1:500 for ICC and 1:10,000 for WB), mouse anti-LAMP1 (DSHB, cat #H4B3, 1:100 for ICC), rat anti-FLAG (Biolegend, cat #637302, 1:100 for ICC), chicken anti-GFP (AvesLab, GFP-1020, 1:1000 for ICC), mouse anti-GFP (Roche, cat #11814460001, 1:10,000 for WB), sheep anti-TGN46 (Biorad, cat #AHP500GT, 1:500 for ICC), rabbit anti-Rab8a (Cell Signaling Technology, cat #6975, 1:500 for ICC), rabbit anti-EEA1 (Cell Signaling Technology, cat #3288, 1:100 for ICC), rabbit anti-Lamtor4 (Cell Signaling Technology, cat#12284, 1:200 for ICC), rabbit anti-RAB10 (Abcam, cat #ab237703, 1:2000 for WB), rabbit anti-RAB10 (phospho-T73) (Abcam, cat #ab23026, 1:300 for ICC and 1:2000 for WB), rabbit anti-RAB12 (Proteintech, cat #18843–1-AP, 1:1000 for WB), rabbit anti-RAB12 (phospho-S106) (Abcam, cat #ab256487, 1:100 for ICC and 1:2000 for WB), rabbit anti-RAB29 (Abcam, cat #ab256526, 1:2000 for WB), rabbit anti-

LRRK2 (Abcam, cat #ab133474, 1:2000 for WB), rabbit anti-LRRK2 (phospho S1292) (Abcam, cat #ab203181, 1:2000 for WB), rabbit anti-cyclophilin B (Abcam, cat #ab16045, 1:2000 for WB), rabbit anti-JIP4 (Cell Signaling Technology, cat#5519, 1:100 for ICC), rabbit anti-LC3B (Cell Signaling Technology, cat#3868, 1:2000 for WB), mouse anti-p62 (Abcam, cat#ab280086, 1:2000 for WB). For staining of the plasma membrane, Phalloidin was used at 1:20 concentration to visualize F-actin (ThermoFisher, cat #A30107).

For ICC, unless otherwise stated, the secondary antibodies were purchased from ThermoFisher. The following secondary antibodies were used: donkey anti-mouse Alexa-Fluor 568 (cat #A10037, 1:500), donkey anti-rabbit Alexa-Fluor 488 (cat #A-21206, 1:500), donkey anti-mouse Alexa-Fluor 568 (cat #A-21202, 1:500), donkey anti-rat Alexa-Fluor 488 (cat #A-21208, 1:500), donkey anti-goat Alexa-Fluor 488 (cat #A-11055, 1:500), donkey anti-rabbit Alexa-Fluor 568 (cat #A10042, 1:500), donkey anti-mouse Alexa-Fluor 647 (cat #A-31571, 1:500), goat anti-rat Alexa-Fluor 647 (cat #A-21247, 1:250–1:500). Donkey anti-chicken Alexa-Fluor 405 (cat #703–475-155, 1:300) was obtained from Jackson ImmunoResearch.

For WB, all secondary antibodies were used at 1:10,000 dilution: IRDyes 800CW Goat anti-Rabbit IgG (Licor, cat #926–32,211) and 680RD Goat anti-Mouse IgG (Licor, cat #926–68,070).

2.6. Confocal microscopy

Confocal images were taken using a Zeiss LSM 880 microscope equipped with a 63 × 1.4 NA objective. Super-resolution imaging was performed using the Airyscan mode. Raw data were processed using Airycan processing in 'auto strength' mode with Zen Black software version 2.3. Only low plasmid expression cells without obvious over-expression artifacts were imaged. For measuring colocalization, Fiji plugin JACoP was used in which Mander's correlation corrected for threshold was used to quantify LRRK2:pRAB colocalization. Colocalized maps were made using the Colocalization Finder plugin in Fiji. For measuring signal intensity, integrated density of each cell was measured using Fiji without thresholding (ImageJ, NIH).

2.7. Immunostaining

HEK293FT cells were fixed with 4% PFA for 10 mins, permeabilized with PBS/ 0.1% Triton for 10 mins and blocked with 5% Donkey Serum (Sigma, cat #D9663) for 1 h at RT. Primary antibodies were diluted in blocking buffer (1% Donkey Serum) and incubated overnight at 4 °C. After three 5 min washes with PBS/ 0.1% Triton, secondary fluorescently labeled antibodies were diluted in blocking buffer (1% Donkey Serum) and incubated for 1 h at RT. Coverslips were washed two times with 1× PBS and an additional 2× with dH_2O, and mounted with ProLong® Gold antifade reagent (ThermoFisher, cat #P10144).

2.8. SDS PAGE and Western Blotting

Proteins were resolved on 4–20% Criterion TGX precast gels (Biorad, cat #5671095) and transferred to nitrocellulose membranes (Biorad, cat #170415) by semi-dry trans-Blot Turbo transfer system (Biorad). The membranes were blocked with Odyssey Blocking Buffer (Licor, cat #927–40,000) and then incubated for 1 h at RT or overnight at 4 °C with the indicated primary antibody. Membranes were simultaneously probed antibodies against a loading reference protein, Cyclophilin B, to allow for accurate relative quantification and ensure equal loading between samples. The membranes were washed in TBST (3 × 5 min) followed by incubation for 1 h at RT with fluorescently conjugated secondary antibodies as stated above (Licor). The blots were washed in TBST (3 × 5 min) and scanned on an ODYSSEY® CLx (Licor). Quantitation of western blots was performed using Image Studio (Licor). All blots presented in each figure panel were derived from the same experiment and were processed in parallel.

2.9. Statistical analysis

Analyses based on cell counts were performed by an investigator blinded to treatment/transfection status. Unpaired student's *t*-tests were used in experiments with two comparable groups, one-way ANOVAs were used for experiments with more than two groups, and two-way ANOVAs were used for experiments where there were two factors in the model. Tukey's *post-hoc* tests were used to determine statistical significance for individual comparisons in those cases where the underlying ANOVA was statistically significant and where all groups' means were compared to every other mean. Unless otherwise stated, graphed data are presented as means ± SD. Comparisons were considered statistically significant where $p < 0.05$. $^{*}p < 0.05$; $^{**}p < 0.01$; $^{***}p < 0.001$; $^{****}p < 0.0001$.

3. Results

3.1. Trapping LRRK2 to Golgi or lysosomal membranes results in enhanced kinase activity

To establish whether membrane targeting is sufficient to activate LRRK2, we generated a series of FRB traps with fluorescence fusion proteins targeting the lysosome using LAMP1 (Fig. 1A); the Golgi using Giantin (Fig. 1F); recycling endosomes using EHD1 (Fig. 1K); early endosomes using Rab5 (Fig. 1P); late endosomes using RAB7 (Fig. 1U); and the plasma membrane using a plasma membrane-targeting sequence (PMTS) from GAP43 (MLCCMRRTKQVEKNDDQKI) (Fig. 1Z). Co-transfection of each of these plasmids with 3xFlag-FKBP-LRRK2 resulted in diffuse cytosolic LRRK2 staining as expected, however, after a 15 min incubation of 200 nM rapamycin, LRRK2 was relocalized to intracellular structures labeled with the trap construct. These signals also colocalized with appropriate endogenous markers of each organelle (Fig. 1). Live imaging of cells expressing either RE-trap or lyso-trap constructs together with a mScarlet-FKBP-LRRK2 construct show this dimerization in real time, with both traps being able to colocalize LRRK2 in a matter of seconds following the addition of rapamycin (Supplementary Fig. 1). Thus, the system employed here is sufficient to rapidly induce partial recruitment of LRRK2 to specified membranes. Importantly, treatment with rapamycin at such a low concentration for 15 min does not induce autophagy in HEK293FT cells (Supplementary Fig. 2A-C).

Having established these tools, we next examined whether recruitment to these membranes was sufficient to increase LRRK2 kinase activity as measured by three molecular readouts: autophosphorylation of LRRK2 at site S1292, pT73 RAB10 and pS106 RAB12. Constructs were transfected into HEK293FT cells and treated with rapamycin in order to evaluate phosphorylation events via Western blot. In each case, the addition of rapamycin resulted in statistically significant increases in S1292 LRRK2 autophosphorylation (Fig. 1B,C; G,H; L, M; Q, R; V,W; a,b) pT73 RAB10 (Fig. 1B,D; G,I; L, N; Q, S; V,X; a,c) and pS106 RAB12 (Fig. 1B,D; G,J; L,O; Q, T; V,Y; a,d) compared to untreated controls. Additionally, treatment of cells with MLi-2 decreased LRRK2 autophosphorylation, RAB10 and RAB12 phosphorylation below baseline levels, demonstrating that the changes in RAB phosphorylation are LRRK2 kinase-dependent. Thus, translocation of LRRK2 to intracellular membranes is sufficient to increase kinase activity and influence RAB substrate phosphorylation, irrespective of membrane identity.

Importantly, rapamycin-treated cells that were transfected with LRRK2 alone did not increase S1292 LRRK2, T73 RAB, nor S106 RAB12 phosphorylation, confirming that LRRK2 kinase activation is dependent on membrane presence and is not a byproduct of the treatment itself (Supplementary Fig. 2D-G). We also conducted a control experiment in which we transfected cells with 3xFLAG-FKBP-LRRK2 and a plasmid containing the FRB domain without any membrane-targeting protein. Under these conditions, cells treated with rapamycin did not have any effect on LRRK2 autophosphorylation nor RAB10 and RAB12

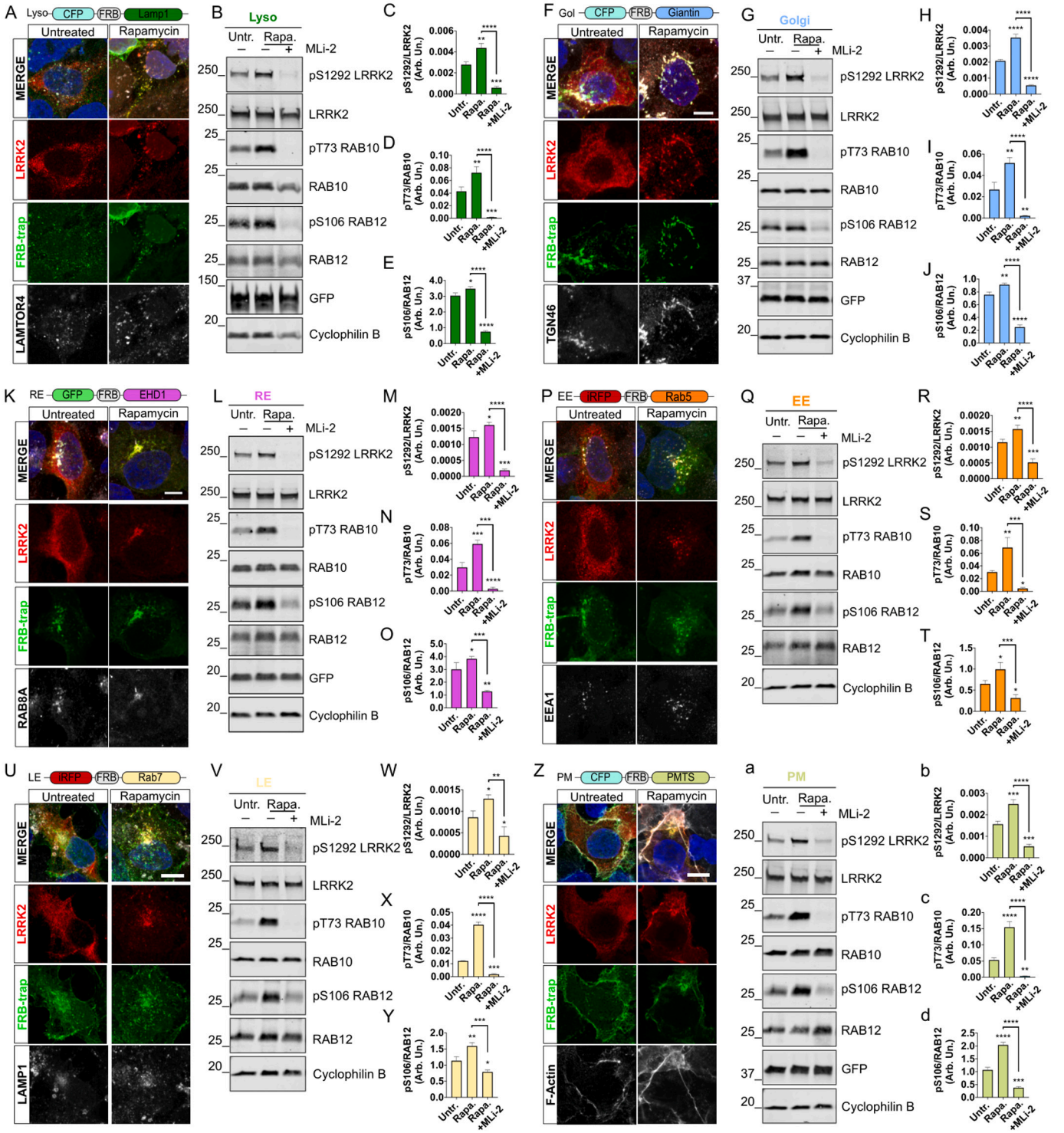

Fig. 1. Recruitment of LRRK2 to multiple intracellular membranes results in activation of LRRK2 kinase activity. Cells were transfected with lysosome (A-E), Golgi (F-J), recycling endosome (K—O), early endosome (P-T), late endosome (U—Y) and plasma membrane (*Z*-d) traps (green) along with FKBP-tagged LRRK2 (red). All trap construct designs are illustrated above each image respectively. Untreated cells were used as negative controls while rapamycin treatment in the absence or presence of MLi-2 were used for recruitment and kinase inhibition of LRRK2 respectively. Endogenous markers for each targeted membrane are shown in grey. Scale bar = 10 μm. Evaluation of pS1292 LRRK2, pRAB10 and pRAB12 are included via Western blot for each trap (B-E, G-J, L-O, Q-T, V—Y, a-d). (C-E, H-J, M-O, R-T, W—Y, b-d): one-way ANOVA with Tukey's post hoc, $^{****}p < 0.0001$, $^{***}p < 0.001$, $^{**}p < 0.01$, $^{*}p < 0.05$, $n = 3$; SD bars shown; (C) $F(2,6) = 116.4$, (D) $F(2,6) = 81.12$, (E) $F(2,6) = 376.3$, (H) $F(2,6) = 323.0$, (I) $F(2,6) = 75.25$, (J) $F(2,6) = 306.8$, (M) $F(2,6) = 104.6$, (N) $F(2,6) = 110.5$, (O) $F(2,6) = 48.55$,(R) $F(2,6) = 69.67$, (S) $F(2,6) = 36.89$, (T) $F(2,6) = 26.02$, (W) $F(2,6) = 22.40$, (X) $F(2,6) = 691.5$, (Y) $F(2,6) = 48.89$, (b) $F(2,6) = 119.8$, (c) $F(2,6) = 154.4$, (d) $F(2,6) = 277.7$. (For interpretation of the references to colour in this figure legend, the reader is referred to the web version of this article.)

phosphorylation, suggesting that it is indeed the presence of a membrane that is critical to heighten LRRK2 kinase activity and is not affected by the binding of LRRK2 to the FRB domain alone (Supplementary Fig. 2H-K).

We next evaluated whether the addition of hyperactive LRRK2 mutations in the ROC (R1441C), COR (Y1699C) and kinase (G2019S) domains of LRRK2 would produce greater activation of LRRK2 signaling than wildtype protein in the context of FKBP-FRB dimerization. We also included a hypothesis testing kinase dead LRRK2 mutant, K1906M, as a negative control. Using the lyso-trap (Fig. 2A), we found that the addition of rapamycin caused a robust increase in pS1292 LRRK2 normalized to total LRRK2 levels which was blocked by MLi-2 (Fig. 2B). Phosphorylation of RAB10 relative to total RAB10 was also increased by rapamycin to similar magnitudes across mutations, with baseline levels being most affected by the R1441C and Y1699C mutations as expected (Fig. 2C). This phosphorylation was significantly reduced with MLi-2 treatment (Fig. 2C). Finally, increased phosphorylation of RAB12 relative to total RAB12 was also noted with wildtype LRRK2 after rapamycin treatment, but not with mutant LRRK2 (Fig. 2D). In all cases, the kinase dead K1906M LRRK2 did not support pRAB10 or pRAB12 activation, demonstrating that these effects on RAB phosphorylation were LRRK2 kinase-dependent.

Similar patterns of LRRK2 activation and RAB phosphorylation were seen using the Golgi-trap construct (Fig. 2E), with the strongest effects on pS1292 LRRK2 found with the G2019S mutation (Fig. 2F) whereas R1441C and Y1699C mutations contributed to the strongest effect on RAB10 phosphorylation (Fig. 2G). Interestingly, increases in pRAB12 were also only observed in rapamycin-treated cells transfected with wildtype LRRK2, with only mild increases observed in the mutant LRRK2 conditions (Fig. 2H). In all cases, inhibition of LRRK2 using MLi-2 or by substitution with the K1906M variant, resulted in minimal activity. These results collectively show either membrane is sufficient in activating LRRK2 kinase, however, divergent patterns of RABs phosphorylation emerge within the context of LRRK2 mutants.

3.2. Phosphorylated RAB proteins accumulate at intracellular membranes via trapped LRRK2

RAB proteins are localized to a variety of intracellular membranes with generally distinct and restricted distributions for each RAB (Homma et al., 2021). Of the two RAB proteins evaluated here, RAB10 has been localized to early endosomes and the endocytic recycling compartment (Babbey et al., 2006; Etoh and Fukuda, 2019; Liu et al., 2013; Štimac et al., 2021) while RAB12 has been found in a variety of vesicular compartments related to endosome function (Efergan et al., 2016; Iida et al., 2005; Matsui et al., 2011; Rydell et al., 2014). As neither RAB is prominently localized to lysosomes or Golgi, we next evaluated the localization of pRABs following the translocation of LRRK2 to these membranes via immunocytochemistry.

As expected, the addition of rapamycin resulted in the redistribution of LRRK2 from diffuse cytosolic expression to structures resembling lysosomes with lyso-trap (Fig. 3A) or Golgi with Golgi-trap (Fig. 3B). In conditions where the lyso-trap was used, pRAB12 staining showed broad colocalization with LRRK2 at lysosomes while pRAB10 was most clearly seen on perinuclear lysosomes after treatment with rapamycin and treatment with MLi-2 diminished the staining of both pRABs. (Fig. 3A). When LRRK2 was directed to the Golgi, pRAB12 was also detected at this organelle, as was pRAB10 although the latter showed only partial localized staining (Fig. 2B). To quantify these effects, we used Mander's coefficient for colocalization between LRRK2 and each pRAB when LRRK2 was translocated to lysosomes (Fig. 3C) and Golgi (Fig. 3D). When comparing between membranes, each pRAB showed similar levels of colocalization with LRRK2, while pRAB12 showed the most colocalization with LRRK2 compared to pRAB10 (Fig. 3E). This finding reinforces the idea that pRAB accumulation consequential to LRRK2 activation is unaffected by membrane identity.

Similarly, relocalizing LRRK2 to perinuclear structures morphologically reminiscent of recycling endosomes resulted in strong staining of pRAB10 and pRAB12 that was blocked by MLi-2 (Fig. 4A). Treatment with rapamycin in the presence of E*E*-trap expression resulted in relocalization of LRRK2 to early endosomes where pRAB10 and pRAB12 levels were also observed (Fig. 4B). Mander's correlation coefficient showed strong colocalization between LRRK2 and pRABs at both early and recycling endosomes (Fig. 4C-F). Thus, LRRK2 can phosphorylate RABs at multiple membranes along the endolysosomal pathway, however, differences in the distribution of pRABs may be visible depending on which membrane LRRK2 is accumulated at.

3.3. JIP4 can be recruited to multiple cellular membranes dependent on LRRK2 kinase activity

Prior studies have suggested that the motor adaptor protein JIP4 can be recruited by phosphorylated RABs to either lysosomes (Bonet-Ponce et al., 2020) or autophagosomes (Boecker et al., 2021) in different cell types. We therefore wanted to test whether LRRK2 could also promote JIP4 recruitment when placed at a variety of membranes within the cell. We found that endogenous JIP4 could be recruited to LRRK2-positive structures using either lyso-trap (Fig. 5A-B), Golgi-trap (Fig. 5C-D), EE-trap (Fig. 5 E-F), or RE-trap (Supplementary Fig. 3A-B). Trap-dependent recruitment of JIP4 was blocked by treatment with MLi-2, consistent with dependence of JIP4 recruitment on RAB phosphorylation. Thus, membrane identity is equally unimportant for JIP4 recruitment once pRABs accumulate at a given membrane.

3.4. RAB29 is not necessary for LRRK2 activation at the lysosome

Although prior data using knockout cells suggests that endogenous RAB29 is not required for LRRK2 activity (Kalogeropulou et al., 2020), it is striking that both LRRK2 and RAB29 knockout mice exhibit prominent lysosomal abnormalities (Kuwahara et al., 2016). Additionally, RAB29 has been characterized as a resident Golgi protein, with overexpression studies showing colocalization to TGN46, GM130 and other known Golgi markers (Beilina et al., 2014; Wang et al., 2014). We therefore examined the potential role of RAB29 in the activation of LRRK2 trapped at the Golgi membrane by knocking down endogenous RAB29 (Fig. 6A), recognising that this would not be possible using approaches to drive LRRK2 to membranes using RAB29 overexpression or RAB9 fusion proteins. Despite the efficient knockdown of RAB29 in which 70–80% of endogenous protein was lost (Fig. 6A, E), we saw no difference in pS1292 LRRK2 between siRNA against RAB29 versus non-targeting control under basal or rapamycin-induced trapping of LRRK2 to the Golgi via Western blot (Fig. 6B). Similar negative results were seen with both pRAB10 (Fig. 6C) and pRAB12 (Fig. 6D). Immunocytochemistry confirmed these results, as no difference in LRRK2 localization was seen in groups transfected with RAB29 compared to NTC siRNA (F). These experiments demonstrate that RAB29 is not required for the activation of LRRK2 in the context of controlled recruitment to the Golgi. Additionally, we evaluated LRRK2 in the proximity of the lysosomal membrane using lyso-trap after RAB29 siRNA knockdown. Similarly, we saw no impairment nor increase in the ability of LRRK2 to translocate to the lysosome following rapamycin treatment, nor was its distribution affected under conditions without rapamycin (Supplementary 3C). More importantly, T73 RAB10 staining in RAB29 siRNA knockdown cells still colocalized to LRRK2 when LRRK2 was translocated to the lysosomal membrane (Supplementary 3C). This suggests that in the absence of RAB29, LRRK2 activation at lysosomes is unaffected and is thus able to phosphorylate RAB10.

4. Discussion

Understanding the mechanisms by which LRRK2 activity is controlled is fundamentally important for discerning the role of this

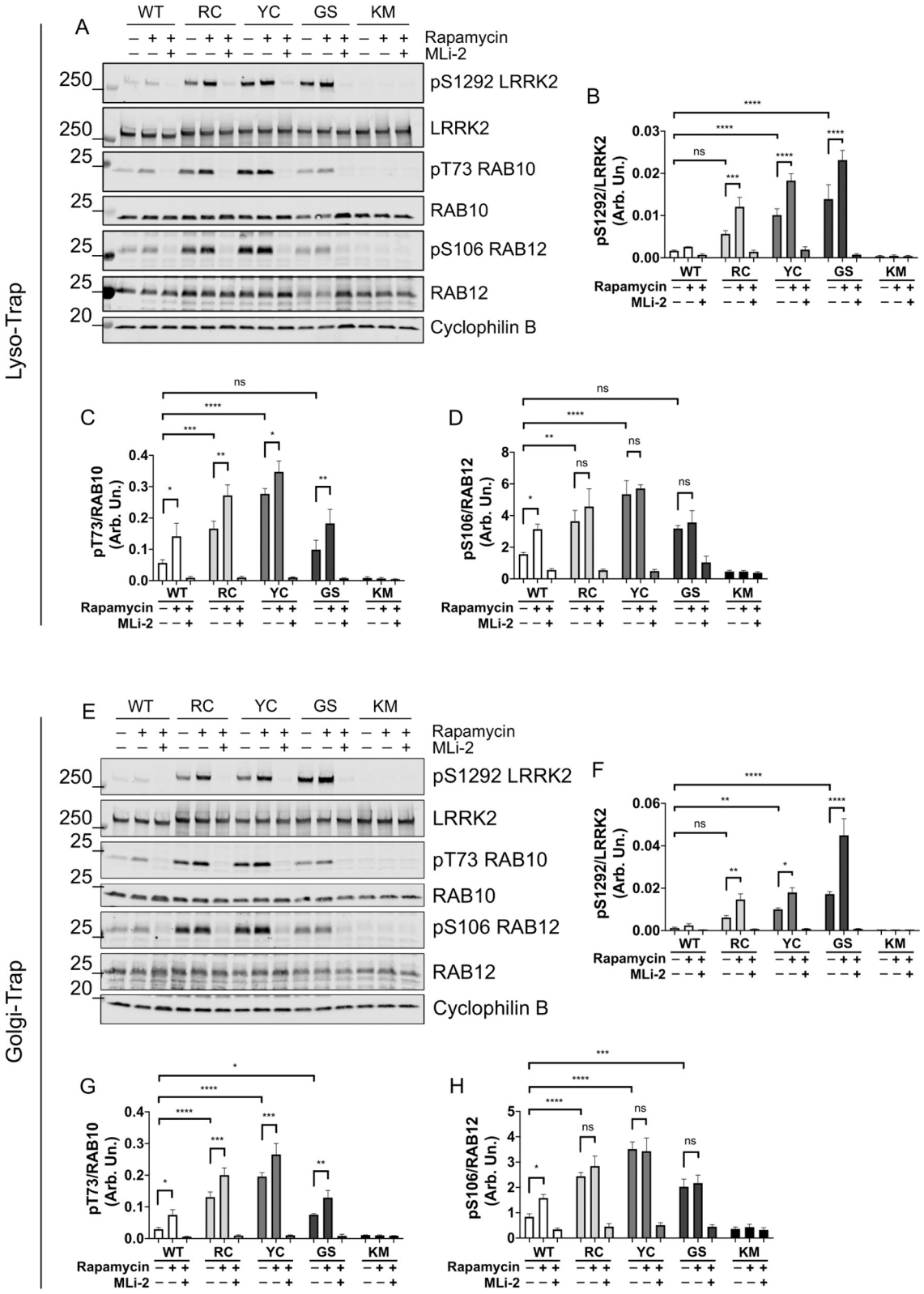

Fig. 2. LRRK2 and RAB10 phosphorylation patterns show additive effects of LRRK2 membrane recruitment and pathogenic mutations. The lyso-trap (A) or Golgi-trap (E) were co-transfected with either WT, R1441C, Y1669C, G2019S, or K1906M LRRK2(-FKBP-3xFlag or mScarlet) varieties and Western blots were run, probing for pS1292 LRRK2, pT73 RAB10, and pS106 RAB12 (B—D, F—H). (B—D, F—H): two-way ANOVA with Tukey's *post-hoc* test, $n = 3$ independent experiments; SD bars shown; (B) treatment, $p < 0.0001$, $F(2,30) = 208.2$; genotype, $p < 0.0001$, $F(4, 30) = 130.8$, (C) treatment, $p < 0.0001$, $F(2, 30) = 200.5$; genotype, $p < 0.0001$, $F(4, 30) = 95.63$, (D) treatment, $p < 0.0001$, $F(2, 30) = 97.52$; genotype, $p < 0.0001$, $F(4, 30) = 45.79$, (E) treatment, $p < 0.0001$, $F(2, 30) = 177.0$; genotype, $p < 0.0001$, $F(4, 30) = 121.5$, (F) treatment, $p < 0.0001$, $F(2, 30) = 310.7$; genotype, $p < 0.0001$, $F(4, 30) = 156.0$, (G) treatment, $p < 0.0001$, $F(2, 30) = 210.1$; genotype, $p < 0.0001$, $F(4, 30) = 117.9$.

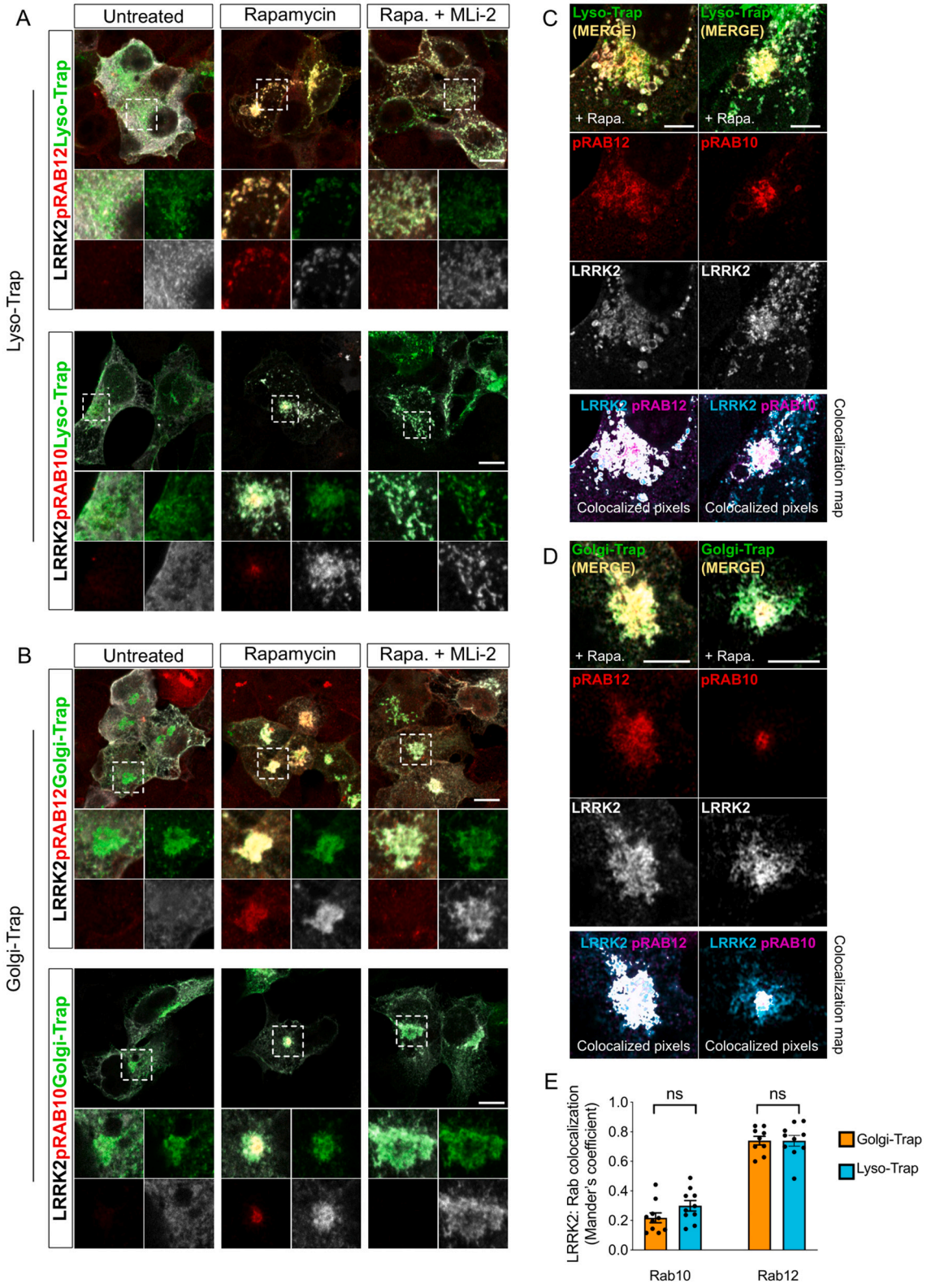

Fig. 3. pT73 RAB10 and pS106 RAB12 are phosphorylated by LRRK2 at the lysosome and Golgi. Utilizing the FRB-FKBP system, representative confocal microscopy images show colocalization of LRRK2 and its RAB substrates at membranes. Using the lyso-trap (A) or the Golgi-trap (B), both pS106 RAB12 and pT73 RAB10 (red) were stained with LRRK2 (grey) and colocalization was measured using airyscan images (C-E) Colocalized pixels are shown for clarity of colocalization. Scale bar = 10 μm (A, B); 5 μm (C, D). E: Quantification of LRRK2:RAB colocalization coefficient from $n = 9$–10 cells for Golgi-trap (orange) and Lyso-trap (cyan) for pRAB10 (left) and pRAB12 (right). One-way ANOVA with Tukey's post hoc analyses: $F(3,35) = 68.18$. Error bars show SEM, ns = not significant. (For interpretation of the references to colour in this figure legend, the reader is referred to the web version of this article.)

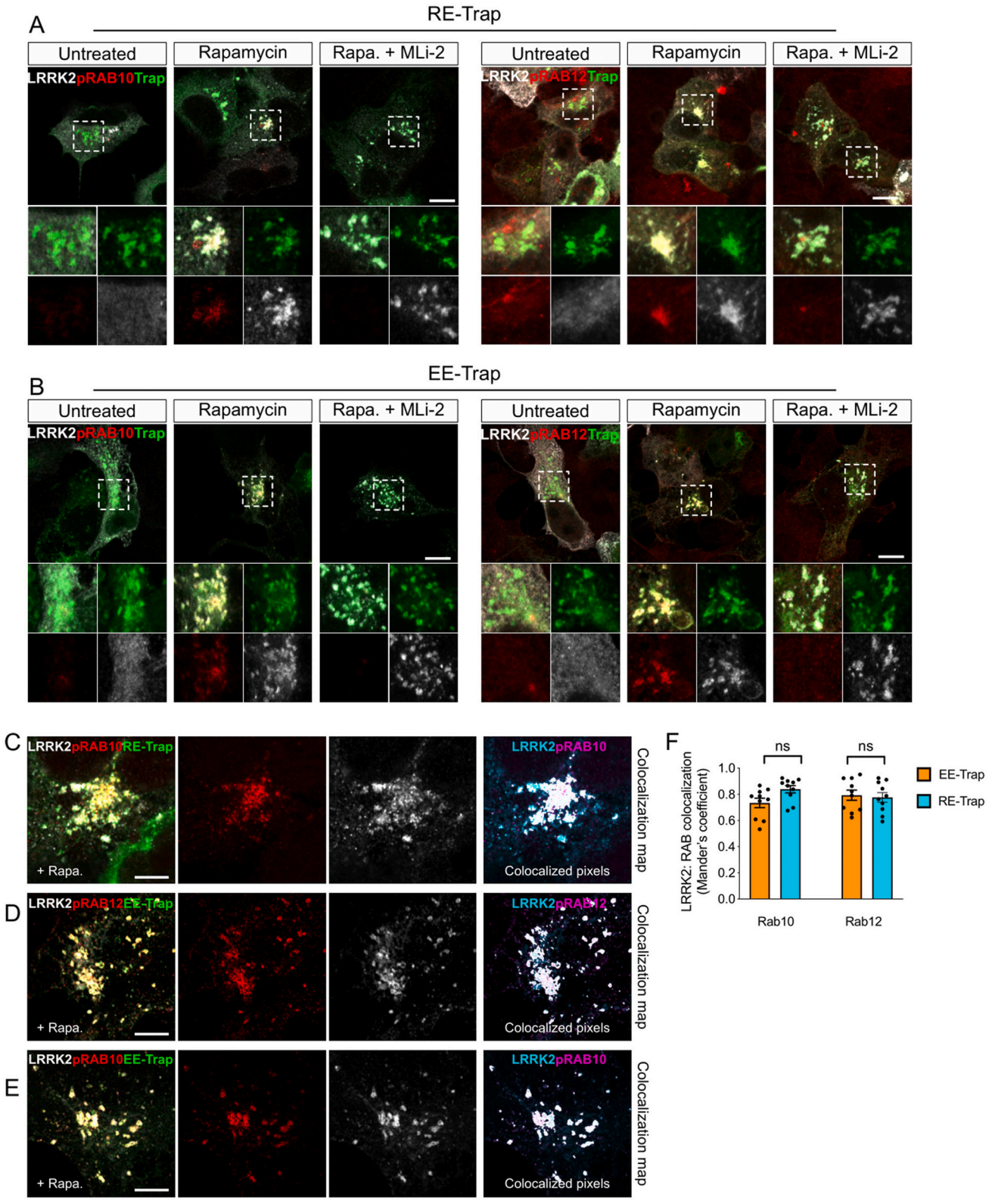

Fig. 4. Colocalization of LRRK2 with pT73 RAB10 and pS106 RAB12 at the early and recycling endosomal membranes. Utilizing the FRB-FKBP system, representative confocal microscopy images show colocalization of LRRK2 and its RAB substrates at the early and recycling endosomal membranes. (A) Using the RE-trap or EE-trap (green), colocalization of pS106 RAB12 and pT73 RAB10 (red) with LRRK2 (grey) were observed when treated with and without rapamycin, and MLi-2 treatment (A-B). Colocalization between LRRK2 and pRABs were measured using airyscan images (C—F). Scale bar = 10 μm (A, B); 5 μm (C-E). F: Quantification of LRRK2:pRAB colocalization coefficient from $n = 10$ cells for EE-trap (orange) and RE-trap (cyan) for pRAB10 (left) and pRAB12 (right). One-way ANOVA with Tukey's post hoc analyses: $F(3,36) = 1.511$. Error bars show SEM, ns = not significant. (For interpretation of the references to colour in this figure legend, the reader is referred to the web version of this article.)

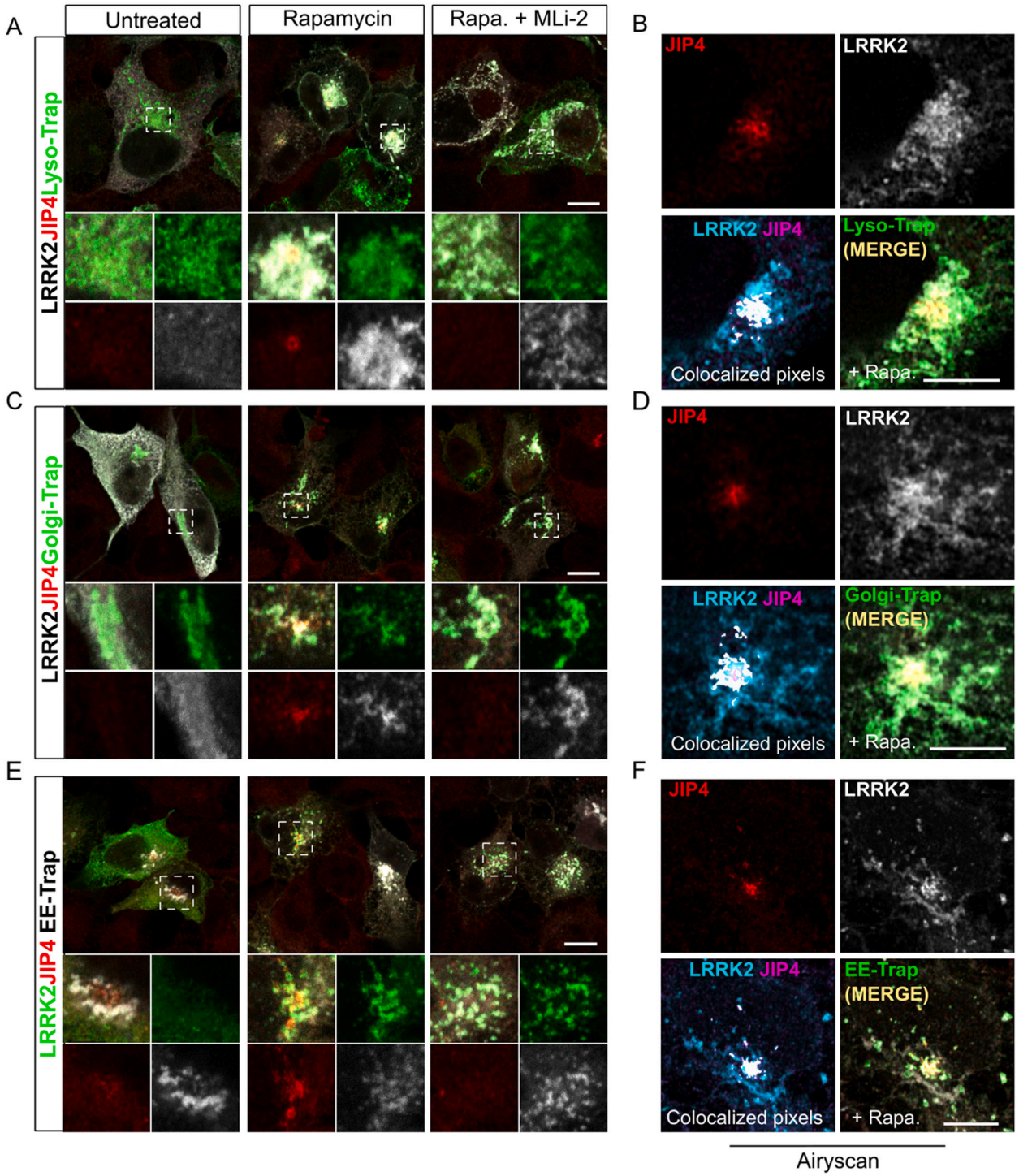

Fig. 5. Recruitment of JIP4 is observed after trapping LRRK2 to the lysosome, Golgi or early endosomes. To investigate whether any events downstream of RAB10 are observed in this trap system, we stained for JIP4 after trapping LRRK2 to the lysosomal (A,B) Golgi (C,D) and early endosome (E,F) membranes under conditions with or without rapamycin or MLi-2 treatments. Airyscan images and colocalization pixels are shown in (B,D,F) for each trap. Scale bar = 10 μm (A, B); 5 μm (C—D). Scale bar = 10 μm (A,C,E); 5 μm (B,D,F).

protein in PD and has strong implications for the clinical application of LRRK2 kinase inhibitors. In the current study, we evaluated whether direction to a variety of endomembranes is sufficient to result in LRRK2 activation, even in the absence of membrane damage. We show that recruitment of LRRK2 to various membranes results in the accumulation of pRABs and recruitment of the effector protein JIP4, regardless of the membrane targeted.

Several prior studies have supported the concept that LRRK2 activation requires membrane targeting, but in the context of either immune signaling and/or membrane damage (Berger et al., 2010; Bonet-Ponce et al., 2020; Eguchi et al., 2018; Herbst et al., 2020). Our study adds to this body of knowledge, showing that once LRRK2 is at any membrane, kinase activation is enhanced, presumably via self-interaction as seen in vitro (Civiero et al., 2012; Greggio et al., 2008; Klein et al., 2009). Our data indicate that membrane damage is not specifically required for LRRK2 activation. Furthermore, all membranes

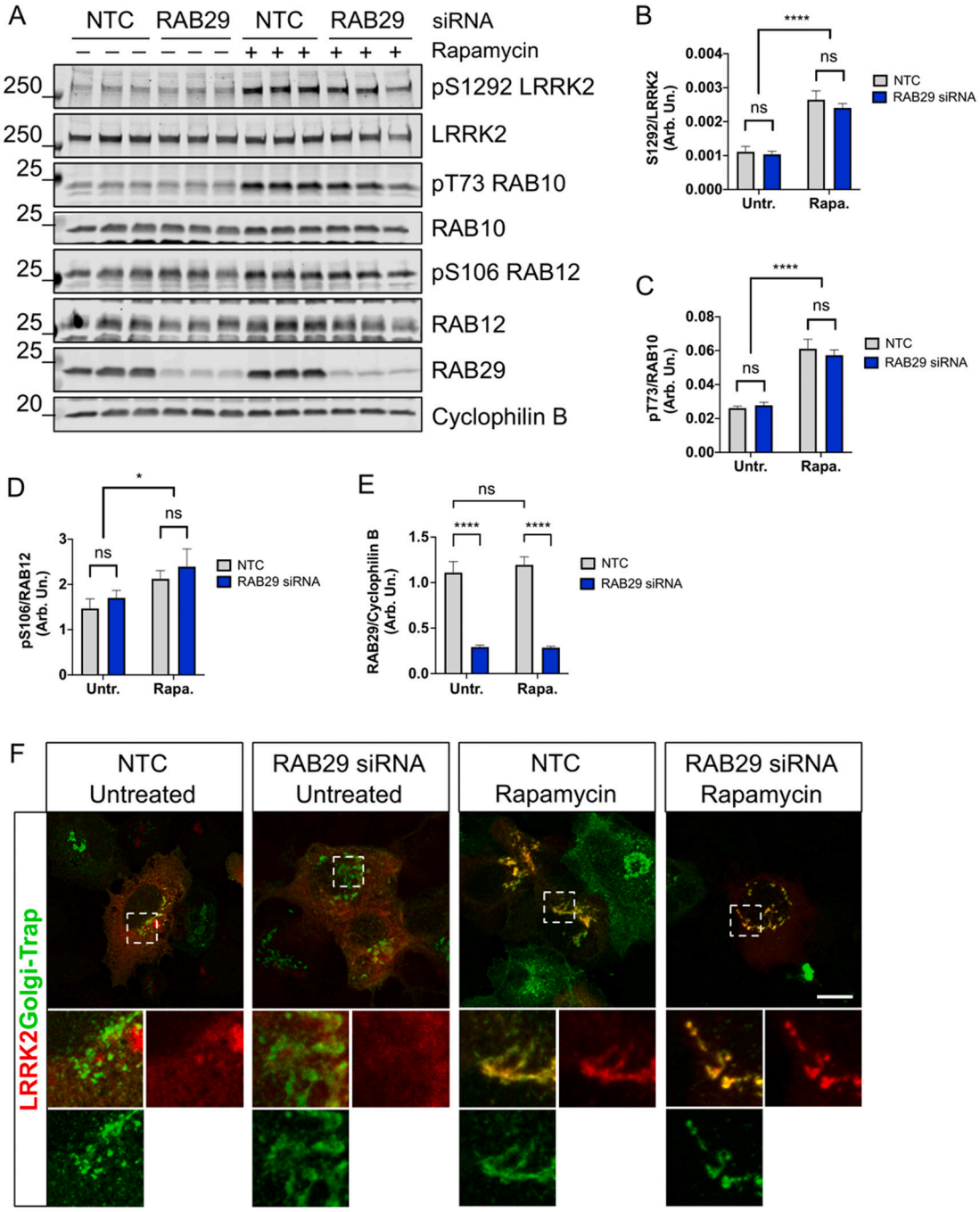

Fig. 6. Knockdown of endogenous RAB29 does not affect LRRK2 activation at the Golgi or lysosomal membranes. Following a 24 h incubation of siRNA RAB29 or non-targeting control, HEK293FT cells were transfected with 3xFlag-FKBP-LRRK2 and Golgi-trap. Cells were then treated with rapamycin for 15 min before lysing and pS1292 LRRK2, pT73 RAB10, and pS106 RAB12 levels were evaluated via Western blot (A-D). RAB29 knockdown efficiency was measured via total levels of endogenous protein (E). (B-E): two-way ANOVA with Tukey's multiple comparisons test, $n = 3$; SD bars shown; (B) treatment, $p < 0.0001$, $F(1, 8) = 214.9$; siRNA, $p = 0.1536$, $F(1, 8) = 2.485$, (C) treatment, $p < 0.0001$, $F(1, 8) = 267.3$; siRNA, $p = 0.6008$, $F(1, 8) = 0.2967$, (D) treatment, $p < 0.0019$, $F(1, 8) = 20.69$; siRNA, $p = 0.1269$, $F(1, 8) = 2.901$, (E) treatment, $p = 0.3936$, $F(1, 8) = 0.8127$; siRNA, $p < 0.0001$, $F(1, 8) = 381.9$.

were equally suitable for activating LRRK2, implying that there are no specific membrane resident proteins involved in LRRK2 activation. Overall, our data are consistent with a model where membrane recruitment is sufficient for LRRK2 activation, although this needs to be tested in future studies. It should be noted that such a model does not exclude that membrane damage and recruitment may both independently contribute to LRRK2 activation.

Interestingly, we also found that once mutant LRRK2 is directed to lysosome or Golgi membranes, phosphorylation of RAB12 is unaffected compared to the robust accumulation of pRAB10. Previous studies have shown that mutant LRRK2 is more prone to accumulate at membranes compared to wildtype protein (Berger et al., 2010; Mamais et al., 2021) and we observed that pRAB12 more strongly colocalized with mutant LRRK2 at membranes compared to pRAB10. Thus, one possible explanation for the minimal effect of membrane-bound mutant LRRK2 on pRAB12 is that mutant LRRK2 is present at membranes prior to induced recruitment. More extensive studies will be needed in order to elucidate differences between mutant LRRK2-dependent RAB phosphorylation.

Prior work has shown that a mitochondrial-targeting sequence fused to the N-terminus of RAB29 is sufficient to direct LRRK2 to mitochondria, increasing its activity and subsequent RAB10 phosphorylation. However, in vivo data from RAB29 knockout mice and in vitro data from RAB29 knockout cells showed no difference in LRRK2 kinase measurements (Gomez et al., 2019; Kalogeropulou et al., 2020). Here, we have confirmed, using the orthogonal approach of siRNA rather than knockout, that RAB29 is not necessary for the activation of LRRK2, as RAB29 deficient cells showed the same magnitude of LRRK2 activation as control cells using LRRK2, RAB10, and RAB12 phosphorylation readouts at both Golgi and lysosomal membranes. Therefore, and in agreement with other recent data, we infer that RAB29 is not an endogenous activator of LRRK2. However, both LRRK2 and RAB29 knockout mice have similar lysosomal phenotypes, suggesting that there is an unresolved pathway relationship between LRRK2 and RAB29 which should be evaluated in future studies.

Collectively, the current results further establish that LRRK2 can be activated by association with multiple endomembranes, resulting in phosphorylation of RABs that then accumulate at local membranes and can recruit effector proteins including JIP4. Additional studies are required to further delineate how LRRK2 becomes activated at endomembranes in cells under pathological conditions.

Supplementary data to this article can be found online at https://doi.org/10.1016/j.nbd.2022.105769.

Author contributions

Conceptualization, L.B-P., M.R.C., J.H.K.; Methodology, L.B-P., J.H.K.; Formal Analysis, J.H.K., L.B-P.; Investigation, J.H.K., L.B-P.; Writing, M.R.C., J.H.K., L.B-P.; Supervision, M.R.C., P.A.L.; Funding, M.R.C., P.A.L.

Declaration of Competing Interest

The authors have no competing interests related to this work.

Acknowledgements

This work was supported by the National Institutes of Health, NIA, Intramural Research Program and the University of Reading. We also thank Rosa Puertollano and Tsukasa Okiyoneda for kindly providing the CFP-FRB-LAMP1 and the EHD1-FRB-GFP plasmids, respectively.

References

Babbey, C.M., Ahktar, N., Wang, E., Chen, C.C.-H., Grant, B.D., Dunn, K.W., 2006. Rab10 regulates membrane transport through early endosomes of polarized Madin-Darby canine kidney cells. Mol. Biol. Cell 17, 3156–3175. https://doi.org/10.1091/mbc.e05-08-0799.

Beilina, A., Rudenko, I.N., Kaganovich, A., Civiero, L., Chau, H., Kalia, S.K., Kalia, L.V., Lobbestael, E., Chia, R., Ndukwe, K., Ding, J., Nalls, M., Olszewski, M., Hauser, D.N., Kumaran, R., Lozano, A.M., Baekelandt, V., Greene, L.E., Taymans, J.-M., Greggio, E., Cookson, M.R., 2014. Unbiased screen for interactors of leucine-rich repeat kinase 2 supports a common pathway for sporadic and familial Parkinson disease. Proc. Natl. Acad. Sci. U. S. A. 111, 2626–2631. https://doi.org/10.1073/pnas.1318306111.

Beilina, A., Bonet-Ponce, L., Kumaran, R., Kordich, J.J., Ishida, M., Mamais, A., Kaganovich, A., Saez-Atienzar, S., Gershlick, D.C., Roosen, D.A., Pellegrini, L., Malkov, V., Fell, M.J., Harvey, K., Bonifacino, J.S., Moore, D.J., Cookson, M.R., 2020. The Parkinson's disease protein LRRK2 interacts with the GARP complex to promote retrograde transport to the trans-Golgi network. Cell Rep. 31, 107614 https://doi.org/10.1016/j.celrep.2020.107614.

Berger, Z., Smith, K.A., Lavoie, M.J., 2010. Membrane localization of LRRK2 is associated with increased formation of the highly active LRRK2 dimer and changes in its phosphorylation. Biochemistry 49, 5511–5523. https://doi.org/10.1021/bi100157u.

Boecker, C.A., Goldsmith, J., Dou, D., Cajka, G.G., Holzbaur, E.L.F., 2021. Increased LRRK2 kinase activity alters neuronal autophagy by disrupting the axonal transport of autophagosomes. Curr. Biol. CB 31, 2140–2154.e6. https://doi.org/10.1016/j.cub.2021.02.061.

Bonet-Ponce, L., Beilina, A., Williamson, C.D., Lindberg, E., Kluss, J.H., Saez-Atienzar, S., Landeck, N., Kumaran, R., Mamais, A., Bleck, C.K.E., Li, Y., Cookson, M.R., 2020. LRRK2 mediates tubulation and vesicle sorting from lysosomes. Sci. Adv. 6 https://doi.org/10.1126/sciadv.abb2454.

Civiero, L., Vancraenenbroeck, R., Belluzzi, E., Beilina, A., Lobbestael, E., Reyniers, L., Gao, F., Micetic, I., De Maeyer, M., Bubacco, L., Baekelandt, V., Cookson, M.R., Greggio, E., Taymans, J.-M., 2012. Biochemical characterization of highly purified leucine-rich repeat kinases 1 and 2 demonstrates formation of homodimers. PLoS One 7, e43472. https://doi.org/10.1371/journal.pone.0043472.

Cookson, M.R., 2010. The role of leucine-rich repeat kinase 2 (LRRK2) in Parkinson's disease. Nat. Rev. Neurosci. 11, 791–797. https://doi.org/10.1038/nrn2935.

Efergan, A., Azouz, N.P., Klein, O., Noguchi, K., Rothenberg, M.E., Fukuda, M., Sagi-Eisenberg, R., 2016. Rab12 regulates retrograde transport of mast cell secretory granules by interacting with the RILP-dynein complex. J. Immunol. Baltim. Md 1950 (196), 1091–1101. https://doi.org/10.4049/jimmunol.1500731.

Eguchi, T., Kuwahara, T., Sakurai, M., Komori, T., Fujimoto, T., Ito, G., Yoshimura, S.-I., Harada, A., Fukuda, M., Koike, M., Iwatsubo, T., 2018. LRRK2 and its substrate Rab GTPases are sequentially targeted onto stressed lysosomes and maintain their homeostasis. Proc. Natl. Acad. Sci. U. S. A. 115, E9115–E9124. https://doi.org/10.1073/pnas.1812196115.

Etoh, K., Fukuda, M., 2019. Rab10 regulates tubular endosome formation through KIF13A and KIF13B motors. J. Cell Sci. 132, jcs226977. https://doi.org/10.1242/jcs.226977.

Fujimoto, T., Kuwahara, T., Eguchi, T., Sakurai, M., Komori, T., Iwatsubo, T., 2018. Parkinson's disease-associated mutant LRRK2 phosphorylates Rab7L1 and modifies trans-Golgi morphology. Biochem. Biophys. Res. Commun. 495, 1708–1715. https://doi.org/10.1016/j.bbrc.2017.12.024.

Funayama, M., Hasegawa, K., Ohta, E., Kawashima, N., Komiyama, M., Kowa, H., Tsuji, S., Obata, F., 2005. An LRRK2 mutation as a cause for the parkinsonism in the original PARK8 family. Ann. Neurol. 57, 918–921. https://doi.org/10.1002/ana.20484.

Gilks, W.P., Abou-Sleiman, P.M., Gandhi, S., Jain, S., Singleton, A., Lees, A.J., Shaw, K., Bhatia, K.P., Bonifati, V., Quinn, N.P., Lynch, J., Healy, D.G., Holton, J.L., Revesz, T., Wood, N.W., 2005. A common LRRK2 mutation in idiopathic Parkinson's disease. Lancet 365, 415–416. https://doi.org/10.1016/S0140-6736(05)17830-1.

Gomez, R.C., Wawro, P., Lis, P., Alessi, D.R., Pfeffer, S.R., 2019. Membrane association but not identity is required for LRRK2 activation and phosphorylation of Rab GTPases. J. Cell Biol. 218, 4157–4170. https://doi.org/10.1083/jcb.201902184.

Greggio, E., Zambrano, I., Kaganovich, A., Beilina, A., Taymans, J.-M., Daniëls, V., Lewis, P., Jain, S., Ding, J., Syed, A., Thomas, K.J., Baekelandt, V., Cookson, M.R., 2008. The Parkinson disease-associated leucine-rich repeat kinase 2 (LRRK2) is a dimer that undergoes intramolecular autophosphorylation. J. Biol. Chem. 283, 16906–16914. https://doi.org/10.1074/jbc.M708718200.

Hammond, G.R.V., Machner, M.P., Balla, T., 2014. A novel probe for phosphatidylinositol 4-phosphate reveals multiple pools beyond the Golgi. J. Cell Biol. 205, 113–126. https://doi.org/10.1083/jcb.201312072.

Herbst, S., Campbell, P., Harvey, J., Bernard, E.M., Papayannopoulos, V., Wood, N.W., Morris, H.R., Gutierrez, M.G., 2020. LRRK2 activation controls the repair of damaged endomembranes in macrophages. EMBO J. e104494 https://doi.org/10.15252/embj.2020104494.

Homma, Y., Hiragi, S., Fukuda, M., 2021. Rab family of small GTPases: an updated view on their regulation and functions. FEBS J. 288, 36–55. https://doi.org/10.1111/febs.15453.

Iida, H., Noda, M., Kaneko, T., Doiguchi, M., Mōri, T., 2005. Identification of rab12 as a vesicle-associated small GTPase highly expressed in Sertoli cells of rat testis. Mol. Reprod. Dev. 71, 178–185. https://doi.org/10.1002/mrd.20294.

Iwaki, H., Blauwendraat, C., Makarious, M.B., Bandres-Ciga, S., Leonard, H.L., Gibbs, J. R., Hernandez, D.G., Scholz, S.W., Faghri, F., Nalls, M.A., Singleton, A.B., 2020. Penetrance of Parkinson's disease in LRRK2 p.G2019S carriers is modified by a polygenic risk score. Mov. Disord. Off. J. Mov. Disord. Soc. https://doi.org/10.1002/mds.27974.

Kalogeropulou, A.F., Freemantle, J.B., Lis, P., Vides, E.G., Polinski, N.K., Alessi, D.R., 2020. Endogenous Rab29 does not impact basal or stimulated LRRK2 pathway activity. Biochem. J. 477, 4397–4423. https://doi.org/10.1042/BCJ20200458.

Klein, C.L., Rovelli, G., Springer, W., Schall, C., Gasser, T., Kahle, P.J., 2009. Homo- and heterodimerization of ROCO kinases: LRRK2 kinase inhibition by the LRRK2 ROCO fragment. J. Neurochem. 111, 703–715. https://doi.org/10.1111/j.1471-4159.2009.06358.x.

Kluss, J.H., Mamais, A., Cookson, M.R., 2019. LRRK2 links genetic and sporadic Parkinson's disease. Biochem. Soc. Trans. BST20180462 https://doi.org/10.1042/BST20180462.

Kumari, U., Tan, E.K., 2009. LRRK2 in Parkinson's disease: genetic and clinical studies from patients. FEBS J. 276, 6455–6463. https://doi.org/10.1111/j.1742-4658.2009.07344.x.

Kuwahara, Tomoki, Inoue, Keiichi, D'Agati, V.D., Fujimoto, T., Eguchi, T., Saha, Shamol, Wolozin, Benjamin, Iwatsubo, Takeshi, Abeliovich, A., Paisan-Ruiz, C., Zimprich, A., Satake, W., Simon-Sanchez, J., Zhang, F.R., Umeno, J., Lewis, P.A., Manzoni, C., Greenman, C., Hassin-Baer, S., MacLeod, D.A., Pihlstrom, L., Bultema, J.J., Pietro, S. M.D., Ma, J., Plesken, H., Treisman, J.E., Edelman-Novemsky, I., Ren, M., Hermann, G.J., Grill, B., MacLeod, D., Plowey, E.D., Cherra, S.J., Liu, Y.J., Chu, C.T., Parisiadou, L., Chan, D., Citro, A., Cordy, J.M., Shen, G.C., Wolozin, B., Beilina, A., Tong, Y., Herzig, M.C., Hinkle, K.M., Tong, Y., Fuji, R.N., Newell-Litwa, K., Seong, E., Burmeister, M., Faundez, V., Dell'Angelica, E.C., Wolozin, B., Gabel, C., Ferree, A., Guillily, M., Ebata, A., Kuwahara, T., Sakaguchi-Nakashima, A., Meir, J.Y., Jin, Y., Matsumoto, K., Hisamoto, N., Currie, E., Dell'Angelica, E.C., Shotelersuk, V., Aguilar, R.C., Gahl, W.A., Bonifacino, J.S., Peden, A.A., Shotelersuk, V., Dell'Angelica, E.C., Hartnell, L., Bonifacino, J.S., Gahl, W.A., Zhen, L., Swank, R.T., Reddington, M., Howlett, O., Novak, E.K., Seong, E., Biskup, S., Steger, M.,

Dell'Angelica, E.C., Ooi, C.E., Bonifacino, J.S., Faundez, V.V., Kelly, R.B., Azevedo, C., Burton, A., Ruiz-Mateos, E., Marsh, M., Saiardi, A., Martin, I., West, A. B., Smith, W.W., Guttentag, S.H., Brenner, S., Saha, S., Kuwahara, T., Tonegawa, R., Ito, G., Mitani, S., Iwatsubo, T., Ito, G., Inoue, K., Inoue, K., 2016. LRRK2 and RAB7L1 coordinately regulate axonal morphology and lysosome integrity in diverse cellular contexts. Sci. Rep. 6, 29945. https://doi.org/10.1038/srep29945.

Lee, A.J., Wang, Y., Alcalay, R.N., Mejia-Santana, H., Saunders-Pullman, R., Bressman, S., Corvol, J.-C., Brice, A., Lesage, S., Mangone, G., Tolosa, E., Pont-Sunyer, C., Vilas, D., Schüle, B., Kausar, F., Foroud, T., Berg, D., Brockmann, K., Goldwurm, S., Siri, C., Asselta, R., Ruiz-Martinez, J., Mondragón, E., Marras, C., Ghate, T., Giladi, N., Mirelman, A., Marder, K., for the Michael J. Fox LRRK2 Cohort Consortium, 2017. Penetrance estimate of *LRRK2* p.G2019S mutation in individuals of non-Ashkenazi Jewish ancestry: *LRRK2* mutation in non-Ashkenazi Jewish ancestry. Mov. Disord. 32, 1432–1438. https://doi.org/10.1002/mds.27059.

Liberles, S.D., Diver, S.T., Austin, D.J., Schreiber, S.L., 1997. Inducible gene expression and protein translocation using nontoxic ligands identified by a mammalian three-hybrid screen. Proc. Natl. Acad. Sci. U. S. A. 94, 7825–7830. https://doi.org/10.1073/pnas.94.15.7825.

Liu, Y., Xu, X.-H., Chen, Q., Wang, T., Deng, C.-Y., Song, B.-L., Du, J.-L., Luo, Z.-G., 2013. Myosin Vb controls biogenesis of post-Golgi Rab10 carriers during axon development. Nat. Commun. 4, 2005. https://doi.org/10.1038/ncomms3005.

Liu, Z., Bryant, N., Kumaran, R., Beilina, A., Abeliovich, A., Cookson, M.R., West, A.B., 2018. LRRK2 phosphorylates membrane-bound Rabs and is activated by GTP-bound Rab7L1 to promote recruitment to the trans-Golgi network. Hum. Mol. Genet. 27, 385–395. https://doi.org/10.1093/hmg/ddx410.

Mamais, A., Kluss, J.H., Bonet-Ponce, L., Landeck, N., Langston, R.G., Smith, N., Beilina, A., Kaganovich, A., Ghosh, M.C., Pellegrini, L., Kumaran, R., Papazoglou, I., Heaton, G.R., Bandopadhyay, R., Maio, N., Kim, C., LaVoie, M.J., Gershlick, D.C., Cookson, M.R., 2021. Mutations in LRRK2 linked to Parkinson disease sequester Rab8a to damaged lysosomes and regulate transferrin-mediated iron uptake in microglia. PLoS Biol. 19, e3001480 https://doi.org/10.1371/journal.pbio.3001480.

Matsui, T., Itoh, T., Fukuda, M., 2011. Small GTPase Rab12 regulates constitutive degradation of transferrin receptor. Traffic Cph. Den. 12, 1432–1443. https://doi.org/10.1111/j.1600-0854.2011.01240.x.

Nalls, M.A., Blauwendraat, C., Vallerga, C.L., Heilbron, K., Bandres-Ciga, S., Chang, D., Tan, M., Kia, D.A., Noyce, A.J., Xue, A., Bras, J., Young, E., von Coelln, R., Simón-Sánchez, J., Schulte, C., Sharma, M., Krohn, L., Pihlstrøm, L., Siitonen, A., Iwaki, H., Leonard, H., Faghri, F., Gibbs, J.R., Hernandez, D.G., Scholz, S.W., Botia, J.A., Martinez, M., Corvol, J.-C., Lesage, S., Jankovic, J., Shulman, L.M., Sutherland, M., Tienari, P., Majamaa, K., Toft, M., Andreassen, O.A., Bangale, T., Brice, A., Yang, J., Gan-Or, Z., Gasser, T., Heutink, P., Shulman, J.M., Wood, N.W., Hinds, D.A., Hardy, J.A., Morris, H.R., Gratten, J., Visscher, P.M., Graham, R.R., Singleton, A.B., 23andMe Research Team, System Genomics of Parkinson's Disease Consortium, International Parkinson's Disease Genomics Consortium, 2019. Identification of novel risk loci, causal insights, and heritable risk for Parkinson's disease: a meta-analysis of genome-wide association studies. Lancet Neurol. 18, 1091–1102. https://doi.org/10.1016/S1474-4422(19)30320-5.

Paisán-Ruíz, C., Jain, S., Evans, E.W., Gilks, W.P., Simón, J., van der Brug, M., López de Munain, A., Aparicio, S., Gil, A.M., Khan, N., Johnson, J., Martinez, J.R., Nicholl, D., Carrera, I.M., Pena, A.S., de Silva, R., Lees, A., Martí-Massó, J.F., Pérez-Tur, J., Wood, N.W., Singleton, A.B., 2004. Cloning of the gene containing mutations that cause PARK8-linked Parkinson's disease. Neuron 44, 595–600. https://doi.org/10.1016/j.neuron.2004.10.023.

Purlyte, E., Dhekne, H.S., Sarhan, A.R., Gomez, R., Lis, P., Wightman, M., Martinez, T.N., Tonelli, F., Pfeffer, S.R., Alessi, D.R., 2018. Rab29 activation of the Parkinson's disease-associated LRRK2 kinase. EMBO J. 37, 1–18. https://doi.org/10.15252/embj.201798099.

Robinson, M.S., Sahlender, D.A., Foster, S.D., 2010. Rapid inactivation of proteins by rapamycin-induced rerouting to mitochondria. Dev. Cell 18, 324–331. https://doi.org/10.1016/j.devcel.2009.12.015.

Ryan, K.J., White, C.C., Patel, K., Xu, J., Olah, M., Replogle, J.M., Frangieh, M., Cimpean, M., Winn, P., McHenry, A., Kaskow, B.J., Chan, G., Cuerdon, N., Bennett, D.A., Boyd, J.D., Imitola, J., Elyaman, W., De Jager, P.L., Bradshaw, E.M., 2017. A human microglia-like cellular model for assessing the effects of neurodegenerative disease gene variants. Sci. Transl. Med. 9 https://doi.org/10.1126/scitranslmed.aai7635.

Rydell, G.E., Renard, H.-F., Garcia-Castillo, M.-D., Dingli, F., Loew, D., Lamaze, C., Römer, W., Johannes, L., 2014. Rab12 localizes to Shiga toxin-induced plasma membrane invaginations and controls toxin transport. Traffic Cph. Den. 15, 772–787. https://doi.org/10.1111/tra.12173.

Sheng, Z., Zhang, S., Bustos, D., Kleinheinz, T., Le Pichon, C.E., Dominguez, S.L., Solanoy, H.O., Drummond, J., Zhang, X., Ding, X., Cai, F., Song, Q., Li, X., Yue, Z., van der Brug, M.P., Burdick, D.J., Gunzner-Toste, J., Chen, H., Liu, X., Estrada, A.A., Sweeney, Z.K., Scearce-Levie, K., Moffat, J.G., Kirkpatrick, D.S., Zhu, H., 2012. Ser1292 autophosphorylation is an indicator of LRRK2 kinase activity and contributes to the cellular effects of PD mutations. Sci. Transl. Med. 4, 164ra161. https://doi.org/10.1126/scitranslmed.3004485.

Singleton, A., Hardy, J., 2011. A generalizable hypothesis for the genetic architecture of disease: pleomorphic risk loci. Hum. Mol. Genet. 20, R158–R162. https://doi.org/10.1093/hmg/ddr358.

Steger, M., Tonelli, F., Ito, G., Davies, P., Trost, M., Vetter, M., Wachter, S., Lorentzen, E., Duddy, G., Wilson, S., Baptista, M.A., Fiske, B.K., Fell, M.J., Morrow, J.A., Reith, A. D., Alessi, D.R., Mann, M., 2016. Phosphoproteomics reveals that Parkinson's disease kinase LRRK2 regulates a subset of Rab GTPases. eLife 5. https://doi.org/10.7554/eLife.12813.

Štimac, I., Jug Vučko, N., Blagojević Zagorac, G., Marcelić, M., Mahmutefendić Lučin, H., Lučin, P., 2021. Dynamin inhibitors prevent the establishment of the cytomegalovirus assembly compartment in the early phase of infection. Life Basel Switz. 11, 876. https://doi.org/10.3390/life11090876.

van Unen, J., Reinhard, N.R., Yin, T., Wu, Y.I., Postma, M., Gadella, T.W.J., Goedhart, J., 2015. Plasma membrane restricted RhoGEF activity is sufficient for RhoA-mediated actin polymerization. Sci. Rep. 5, 14693. https://doi.org/10.1038/srep14693.

Varnai, P., Thyagarajan, B., Rohacs, T., Balla, T., 2006. Rapidly inducible changes in phosphatidylinositol 4,5-bisphosphate levels influence multiple regulatory functions of the lipid in intact living cells. J. Cell Biol. 175, 377–382. https://doi.org/10.1083/jcb.200607116.

Wang, S., Ma, Z., Xu, X., Wang, Z., Sun, L., Zhou, Y., Lin, X., Hong, W., Wang, T., 2014. A role of Rab29 in the integrity of the trans-Golgi network and retrograde trafficking of Mannose-6-phosphate receptor. PLoS One 9, e96242. https://doi.org/10.1371/journal.pone.0096242.

West, A.B., 2014. Ten years and counting: moving leucine-rich repeat kinase 2 inhibitors to the clinic. Mov. Disord. Off. J. Mov. Disord. Soc. https://doi.org/10.1002/mds.26075.

Willett, R., Martina, J.A., Zewe, J.P., Wills, R., Hammond, G.R.V., Puertollano, R., 2017. TFEB regulates lysosomal positioning by modulating TMEM55B expression and JIP4 recruitment to lysosomes. Nat. Commun. 8 (1), 1580.

Zimprich, A., Biskup, S., Leitner, P., Lichtner, P., Farrer, M., Lincoln, S., Kachergus, J., Hulihan, M., Uitti, R.J., Calne, D.B., Stoessl, A.J., Pfeiffer, R.F., Patenge, N., Carbajal, I.C., Vieregge, P., Asmus, F., Müller-Myhsok, B., Dickson, D.W., Meitinger, T., Strom, T.M., Wszolek, Z.K., Gasser, T., 2004. Mutations in LRRK2 cause autosomal-dominant parkinsonism with pleomorphic pathology. Neuron 44, 601–607. https://doi.org/10.1016/j.neuron.2004.11.005.